Identification of a Loss-of-Function Mutation in *Ube2l6* Associated With Obesity Resistance

Genevieve Marcelin,[1] Shun-Mei Liu,[1] Gary J. Schwartz,[1,2] and Streamson C. Chua, Jr.[1,2]

We previously mapped a locus on BALB/c chromosome 2 associated with protection from leptin-deficiency–induced obesity. Here, we generated the corresponding congenic mouse strain by introgression of a segment of C57BL/6J chromosome 2 to the BALB/c background to confirm the genotype–phenotype associations. We found that the BALB/c alleles decreased fat mass expansion by limiting adipocyte hyperplasia and adipocyte hypertrophy. This was concomitant to an increase in adipocyte triglyceride lipase (ATGL)-mediated triglyceride breakdown and prolongation of ATGL half-life in adipose tissue. In addition, BALB/c alleles on chromosome 2 exerted a cell-autonomous role in restraining the adipogenic potential of preadipocytes. Within a 9.8-Mb critical interval, we identified a nonsynonymous coding single nucleotide polymorphism in the gene coding for the ubiquitin-conjugating enzyme E2L6 (*Ube2l6*, also known as *Ubch8*) and showed that the BALB/c allele of *Ube2l6* is a hypomorph leading to the lack of UBE2L6 protein expression. *Ube2l6* knockdown in 3T3-L1 adipocytes repressed adipogenesis. Thus, altered adipogenic potential caused by *Ube2l6* knockdown is likely critically involved in BALB/c obesity resistance by inhibiting adipogenesis and reducing adipocyte numbers. Overall, we have identified a loss-of-function mutation in *Ube2l6* that contributes to the chromosome 2 obesity quantitative trait locus. ***Diabetes*** **62:2784–2795, 2013**

The ability of white adipose tissue (WAT) depots to store energy as triglycerides (TGs) packed into lipid droplets represents a pivotal mechanism allowing for fuel storage and maintenance of organismal homeostasis in mammals. TG hydrolysis supplies energy for the whole organism during periods of negative energy balance, whereas lipogenesis is promoted during positive energy balance states (1). The ratio between lipolysis and lipogenesis controls fat build-up and is dynamically controlled by multiple hormonal signals. Catecholamines and leptin, among other regulators, maintain a catabolic mode by promoting lipolysis (2,3) and antagonizing lipogenesis (4), whereas insulin has an anabolic role (5,6). Thus, lipogenic pathways are markedly induced in the adipose tissue of C57BL6/J leptin-deficient animals (7), leading to increased fat mass attributable to the hypertrophy of preexisting adipocytes and the generation of new adipocytes from immature adipocytes or local precursor cells (8,9). Various lines of evidence indicate that adipocyte hyperplasia could be a factor in the development of obesity (10,11).

From the [1]Department of Medicine, Albert Einstein College of Medicine, Bronx, New York; and the [2]Department of Neuroscience, Albert Einstein College of Medicine, Bronx, New York.
Corresponding author: Streamson C. Chua, Jr., streamson.chua@einstein.yu.edu.
Received 3 August 2012 and accepted 28 March 2013.
DOI: 10.2337/db12-1054

In this setting, we recently identified that the BALB/c mouse genome carried alleles protecting against obesity, as compared with the C57BL6/J mouse genome, and further linked BALB/c leanness to the quantitative trait locus (QTL) *Lipq1* (for lipolytic line QTL 1) located on chromosome 2. Specifically, the QTL repressed fat mass expansion that was associated with decreased adipocyte size and number (12). Here, we generated a congenic strain with an introgressed segment of chromosome 2 containing the C57BL/6J *Lipq1* allele on the BALB/c genetic background that permitted us to uncover a previously unknown role of the ubiquitin-conjugating enzyme E2L6 (UBE2L6) in adipocyte physiology.

RESEARCH DESIGN AND METHODS

Animals. Congenic strain at the generation N4 (i.e., ~93.8% of BALB/c background) were produced by repeated backcrosses to an inbred BALB/c strain obtained from Jackson Laboratory, with selection for C57BL6/J-BALB/c heterozygous haplotype on chromosome 2. Allelic constitution of chromosome 2 was determined using microsatellites markers and analysis of single nucleotide polymorphism (SNP) as follows: *D2Mit37* (74.49 Mb; forward: 5′- tgtgcaagccagaaaagttg-3′; reverse: 5′- gaaggggattgtaaattggtacc-3′); *rs6303737* (79.18 Mb; forward: 5′- acgttgaagaaggcaaacca-3′; reverse: 5′- tgtttatgggac tcctgaatg-3′; Dpn1); *rs28046677* (83.25 Mb; forward: 5′- gcttttcctcttgtatcag gttg-3′; reverse: 5′- gctccagtcctgcagatgat-3′; *Hae*III); rs3710636 (89.00 Mb; forward: 5′- ctccctggttgcttccaata-3′; reverse: 5′- gaatacaagaagcacactgcaaa-3′; Msp1); rs13459164 (94.35 Mb; forward: 5′- gacagaagaggtggcgttgt-3′; reverse: 5′- tg cttaccttgctctgaagaa-3′; Msp1); *D2Mit12* (102.90 Mb; forward: 5′- ctacttccc aggtgcttgga-3′; reverse: 5′- tccaaagaactgaatggaca-3′), *D2Mit42* (104.41 Mb; forward: 5′- attactgggcaggaacatttg-3′; reverse: 5′- gccaaacttccagactcctc-3′); *D2Mit63* (117.68 Mb; forward: 5′-gcagtctaccaggagcaacc-3′; reverse: 5′- tgga tgtaggcatgtgcct-3′).

N2 *ob/+Agrp*$^{-/-}$ (generated from F1 *ob/+Agrp*$^{-/-}$ X N5 BALB/c *ob/+Agrp*$^{-/-}$) were backcrossed three times with BALB/c mice and N4 *ob/+ Agrp*$^{+/-}$ were intercrossed to compare N4 BALB.2^{CC} and N4 BALB.2^{BC} *ob/ob Agrp*$^{-/-}$ littermates fed with chow diet (Labdiet 5001; kcal %: protein, 28.5%; fat, 13.5%; carbohydrates, 58%). Lean N4 BALB.2^{cc} and N4 BALB.2^{BC} *ob/+* or *ob*$^{+/+}$ *Agrp*$^{-/-}$ were fed a high-fat diet (Research diet D12451; kcal %: protein, 20%; fat, 45%; carbohydrates, 35%). All procedures were reviewed and approved by the institution's animal care committee.

Body composition and indirect calorimetry. Body composition was measured by magnetic resonance spectroscopy using an EchoMRI (Echo Medical Systems). Fat mass percentage was calculated as the ratio between fat mass and body weight. Metabolic measurements (oxygen consumption, respiratory exchange ratio, locomotor activity, food intake) were obtained continuously using a CLAMS (Columbus Instruments) open-circuit indirect calorimetry system.

Histological analysis of adipose tissue and estimation of adipocytes number per fat pad. Adipocyte sizes and number were determined as previously described (13,14).

Ex vivo lipolysis. Glycerol and fatty acids released from fat explants were determined as previously described (12).

RNA quantification by RT-PCR. RNA was prepared from C57BL6/J *ob/ob* and BALB/c *ob/ob* adipose tissue using QiagenRNeasy tissue kit (Qiagen). cDNA was synthesized using SuperScript III and random hexamers (Invitrogen). Amplification of whole *Ube2l6* cDNA was performed with (forward) 5′-atg atggccagcaagcgagtgg-3′ and (reverse) 5′-ttaagagggccggtccactccgaa-3′. Quantitative PCR was performed with the following primer sets: *Atgl* (forward: 5′-tgaccatctgccttccag a-3′; reverse: 5′-tgtaggtggcgcaagaca-3′), *Ppar*γ (forward: 5′-aagacaacggacaaatca cca-3′; reverse: 5′-gggggtgatatgtttgaacttg-3′), *Ap2* (forward: 5′-ggatggaaagtcgaccacaa-3′; reverse: 5′-tggaagtcacgcctttcata-3′), *Hsl*

(forward: 5′-gcgctggaggagtgttttt-3′; reverse: 5′-ccgctctccagttgaacc-3′), *Ube2l6* (forward: 5′-aagcgagtggcgaaagag-3′; reverse: 5′-tttgaggccatagggaag c-3′), and *β-actin* (forward: 5′-ctggagaagagctatgagctgcct-3′; reverse: 5′-ctcctgcttgctgatcc acatctg-3′).

Culture of adipose tissue explants. Organ culture was performed as previously described (15,16). Briefly, freshly dissected subcutaneous fat pad from *ob/ob* mice were minced and placed in M199 medium supplemented with insulin (1 mU/mL) and dexamethasone (30 nmol/L) and incubated in a humidified incubator maintained at 37°C with 5% CO_2. To analyze adipocyte TG lipase (ATGL) protein turnover, cycloheximide (CHX) with or without MG-132 was added to the culture medium. After 5 h of culture, samples were processed for protein analysis.

Primary stromal vascular cell differentiation to adipocytes. Adipose stromal vascular (SV) cells were isolated from WAT of lean wild-type male mice and digested with 1 mg/mL collagenase D (Roche). SV cells were amplified in DMEM supplemented with 10 ng/mL basic fibroblast growth factor and 10% calf serum. After 72 hours, adipose SV cells were seeded at the same density and grown to reach confluence. After adipogenic induction (DMEM supplemented with 10% FBS, 0.25 μg/mL Dexamethasone, 0.5 mmol/L isobutylmethylxanthine, and 1 μg/mL insulin) for 72 h, cultures were maintained in DMEM 10% FBS and insulin.

Metabolites and hormone concentration determination. Samples were collected from mice either fed ad libitum or fasted overnight (~15 h). Glycemia was determined using a glucometer (Abbott), serum insulin levels using ELISA (Linco Mouse Insulin kit), plasma free fatty acids (FFA; Wako) and serum glycerol (Cayman) using a colorimetric assay.

Immunoblot analysis. Protein extracts were prepared as previously described (12). Immunoblots were incubated with primary antibodies against hormone-sensitive lipase (HSL), peroxisome proliferator–activated receptor PPARγ, ATGL, β-actin (Cell Signaling), AP2 (R&D), and UBE2L6 (Santa Cruz).

Expression profiling. RNA quality was assessed with Agilent Bioanalyzer 2100. The amplification and hybridization on the Affymetryx Mouse Gene 1.0 ST were performed by the core facility of Albert Einstein College of Medicine. Raw data were normalized using the robust multi-array average algorithm using the Affymetryx Expression Console Software 1.1 and data from two independent replicates (each replicate represents a pool of three individuals) were used to assess expression differences between the two strains. Differentially expressed probe sets were considered as those with a coefficient of variation <0.5 and $P < 0.05$ (t test).We used uncorrected t test to err on the side of false-positive results rather than risk false-negative results. We filtered out low expression signal for genes with signal below the detection error (indicating no or low expression), and cut-off of 32 (mean ± 2 SD) was calculated from negative controls.

In silico assessment of nonsynonymous polymorphism functionality. SIFT scores (http://sift.bii.a-star.edu.sg/) classify amino acid substitution as deleterious (0.00–0.05), potentially intolerant (0.0051–0.10), borderline (0.101–0.20), or tolerant (0.201–1.00) (17).

Cell transfection and allele-specific protein stability assay. The vector containing *Ube2l6* cDNA was obtained from Addgene (#12440) (18) and targeted mutagenesis, verified by sequencing, was used to produce the BALB-*Ube2l6* allele. 3T3 fibroblasts or B16 cells were transfected: 48 h after DNA/lipofectamine 2000 (Invitrogen) complex exposition, cells were processed for protein analysis or incubated with the translation inhibitor CHX (1 μg/mL).

3T3-L1 cell culture and *Ube2l6* knockdown. 3T3-L1 preadipocytes were differentiated as previously described (19). Knockdown of *Ube2l6* used *Ube2l6* shRNA lentiviral particles (Santa Cruz). Briefly, 3T3-L1 preadipocytes were plated into 12-well plates and incubated with sh*Ube2l6* or sh*Control* (encoding a scrambled shRNA as a negative control) lentiviral particles (5×10^5 particles/mL) in medium containing 8 μg/mL polybrene. Transduction was maintained for 16 h. Puromycin selection (2 μg/mL) was performed starting 24 h after infection and was maintained during experiment.

Statistical analysis. Results are shown as average ± SEM. Comparisons between groups for indirect calorimetry were performed by two-way repeated measures ANOVA, with genotype and time as factors. Unpaired Student t test was performed as indicated in the figures. Significance was accepted at $P < 0.05$. Statistical analysis was performed with GraphPad Prism 5.

RESULTS

BALB/c alleles on chromosome 2 suppress obesity and glucose intolerance and promote fatty acid oxidation. We previously mapped a locus on BALB/c chromosome 2 associated with protection from leptin-deficiency–induced obesity. Here, we set out to determine if this locus acted autonomously to affect obesity susceptibility. We derived a congenic strain by introgression of a subregion from C57BL6/J chromosome 2 extending from 74.5 to 122.2 Mb into BALB/c (BALB) mice. BALB.2^{BC} (heterozygous haplotype) and BALB.2^{CC} mice (homozygous BALB/c haplotype) were compared in the context of leptin deficiency and diet-induced obesity. As previously described, mice were *Agrp*$^{-/-}$ (20) to lower glucose and insulin levels, which are confounding factors in obesity studies (12).

At 2 months of age, BALB.2^{BC} *ob/ob* males and females displayed a significant increase in body weight compared with BALB.2^{CC} *ob/ob* littermates because of increased fat mass deposition (+40%) (Fig. 1*A*). Similar effects were observed in BALB.2^{BC} diet-induced obesity congenic mice with enhanced fat deposition (10.2 ± 1.36 vs. 13.8 ± 0.79 g of fat mass [$P = 0.04$] in BALB.2^{CC} and BALB.2^{BC} males, respectively) mirrored by decreased lean mass growth (27.7 ± 1.33 vs. 24.0 ± 0.83 g of lean mass [$P = 0.035$] in BALB.2^{CC} and BALB.2^{BC} males, respectively) compared with diet-induced obesity BALB.2^{CC} mice.

Indirect calorimetry revealed that BALB.2^{CC} *ob/ob* leanness was associated with decreased respiratory exchange ratio values (Fig. 1*B*), indicating increased use of FFA relative to carbohydrates. VO_2 consumption (Fig. 1*C*), activity (Fig. 1*D*), and caloric intake (Fig. 1*E*) were similar between BALB.2^{CC} *ob/ob* and BALB.2^{BC} *ob/ob*.

Concerning glucose homeostasis, we found comparable fasting glucose levels in BALB.2^{BC} and BALB.2^{CC} *ob/ob* mice (231.3 ± 34.97 vs. 218.0 ± 21.06 mg/dL of glucose [$P = 0.78$] in BALB.2^{CC} and BALB.2^{BC} males, respectively) and increased insulin levels in BALB.2^{CC} *ob/ob* mice (25.0 ± 3.02 vs. 6.38 ± 1.48 ng/mL of insulin [$P = 0.0008$] in BALB.2^{CC} and BALB.2^{BC} males, respectively). A glucose tolerance test revealed impaired glucose clearance in BALB.2^{BC} *ob/ob* compared with BALB.2^{CC} *ob/ob* mice (Fig. 1*F*). Accordingly, an insulin tolerance test showed that BALB.2^{BC}*ob/ob* mice were more insulin-resistant (Fig. 1*G*). Thus, BALB.2^{BC} mice displayed an increased propensity for development of obesity associated with glucose intolerance.

BALB/c alleles on *Lipq1* enhanced TG mobilization and ATGL protein stability. Histological analysis of WAT (Fig. 2*A*) showed decreased fat mass in BALB.2^{CC} versus BALB.2^{BC}*ob/ob* mice (Fig. 2*B*) resulting from smaller adipocytes (Fig. 2*C*) and decreased adipocytes number (Fig. 2*D*).

With regard to the lower respiratory exchange ratio values and adipocyte hypotrophy observed in the BALB.2^{CC} *ob/ob* mice, we have measured the levels of FFA and glycerol in mice fed ad libitum to characterize the metabolic changes underlying BALB/c obesity resistance. Both FFA (Fig. 2*E*) and glycerol (Fig. 2*G*) were elevated in BALB.2^{CC} ob/ob. When fasted, only FFA levels were elevated in BALB.2^{CC} (Fig. 2*F* and 2*H*). Moreover, basal glycerol release from WAT explants indicated that BALB.2^{CC} *ob/ob* mice displayed higher lipolysis rates compared with BALB.2^{BC}*ob/ob* mice (Fig. 2*I*).

In adipocytes, ATGL and HSL activity account for 95% of the TG hydrolysis activity (21), and we have further investigated the relative contribution of each enzyme. Lipolysis in WAT explants isolated from BALB.2^{CC}*ob/ob* and BALB.2^{BC} *ob/ob* mice was determined in the absence and presence of the HSL inhibitor CAY10499 (22), which allowed us to measure total and ATGL-mediated lipolysis, respectively. FFA release by BALB.2^{CC} *ob/ob* explants was higher in both conditions (Fig. 2*J*). However, the extent of the difference in lipolysis between BALB.2^{CC} and BALB.2^{BC} genotypes (i.e., ΔFFA release) was greater in the basal condition than after CAY10499 treatment (496.4 ± 91.2

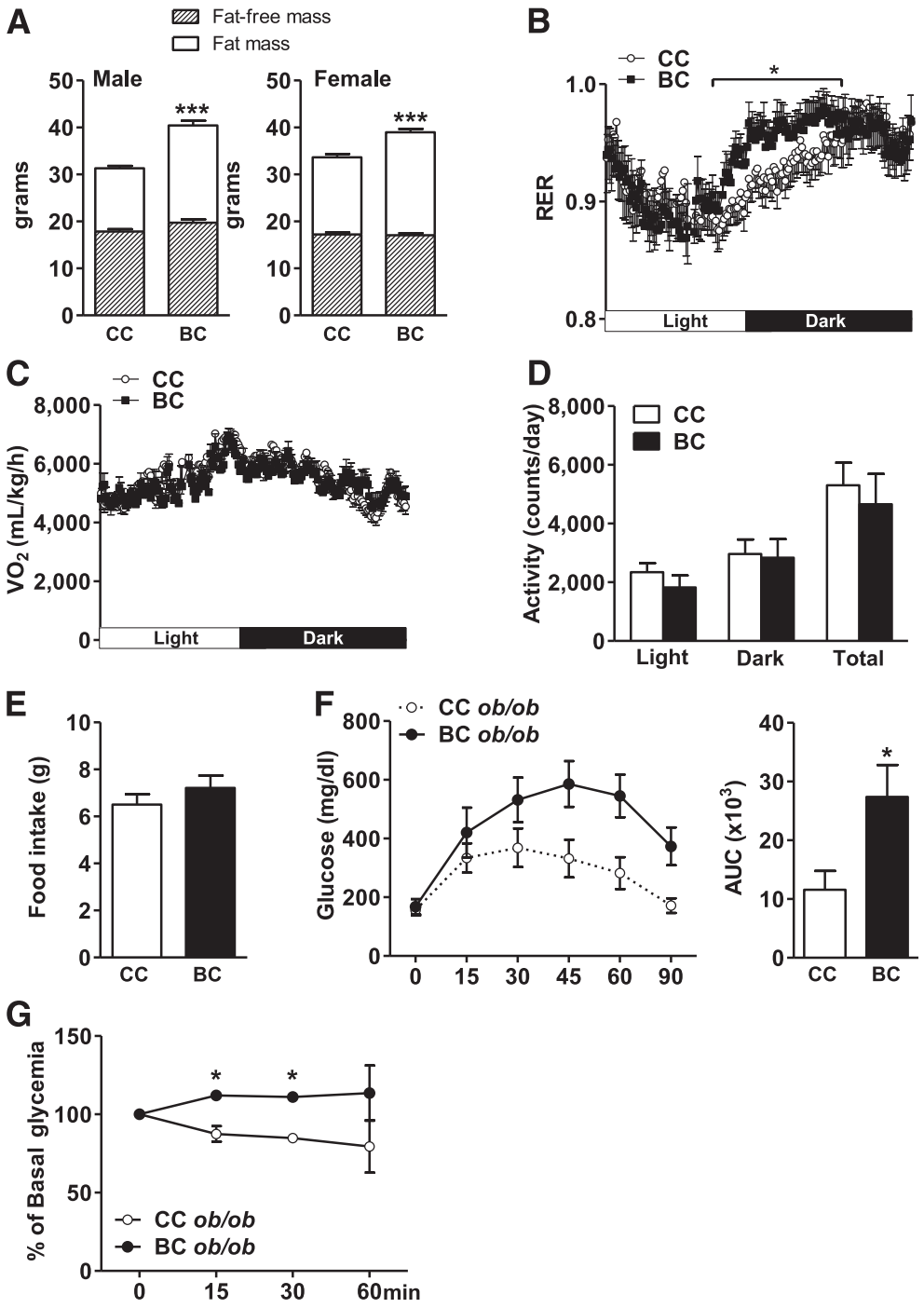

FIG. 1. BALB.2^{BC}*ob/ob* mice displayed increased obesity susceptibility associated with altered glucose clearance and increased fatty acid oxidation. *A*: Body composition (fat mass and fat-free mass) were analyzed in leptin-deficient BALB.2^{CC} and BALB.2^{BC} males and females at age 2 months (n = 7–10). Respiratory exchange ratios (RER; *B*), oxygen consumption normalized to fat-free mass (*C*), spontaneous locomotor activity (*D*), and daily food intake (*E*) were determined during light and dark cycles in BALB.2^{CC} and BALB.2^{BC}*ob/ob* mice with free access to chow diet (n = 4). *F*: Glucose tolerance test (GTT) was performed by measuring blood glucose concentration after an overnight fast at the indicated times after intraperitoneal injection of glucose (1 mg/g body weight) in BALB.2^{CC} and BALB.2^{BC} *ob/ob* mice and the glucose area under the curve (AUC) was calculated (n = 4). *G*: Insulin tolerance test was performed after 6 h of fast with 3 U/kg insulin in BALB.2^{CC} and BALB.2^{BC}*ob/ob* mice (n = 4). Glucose concentration is expressed as % of basal glycemia. Data are expressed as average ± SEM. Unpaired t tests (*A*, *D*, *E*, *F*) and two-way ANOVA tests (*B*, *C*) were performed. *$P < 0.05$. ***$P < 0.0005$.

vs. 245.8 ± 44.4 in basal and CAY10499-treated conditions; $P = 0.0307$), indicating that the increased TG breakdown observed in BALB.2^{CC} *ob/ob* adipose tissue relied on enhanced activity of HSL and ATGL. In addition, ATGL expression was upregulated in BALB.2^{CC}*ob/ob* mice (Fig. 3*D*), whereas total HSL concentration was unchanged despite increased phospho Ser660-HSL in BALB.2^{CC} versus BALB.2^{BC} *ob/ob* (data not shown). However, with regard to the expression of these two lipases in BALB/c *ob/ob* mice (12), we reasoned that the pathways that are under direct control of genetic determinants on chromosome 2 should be replicated in congenic lines and in parental strains (23).

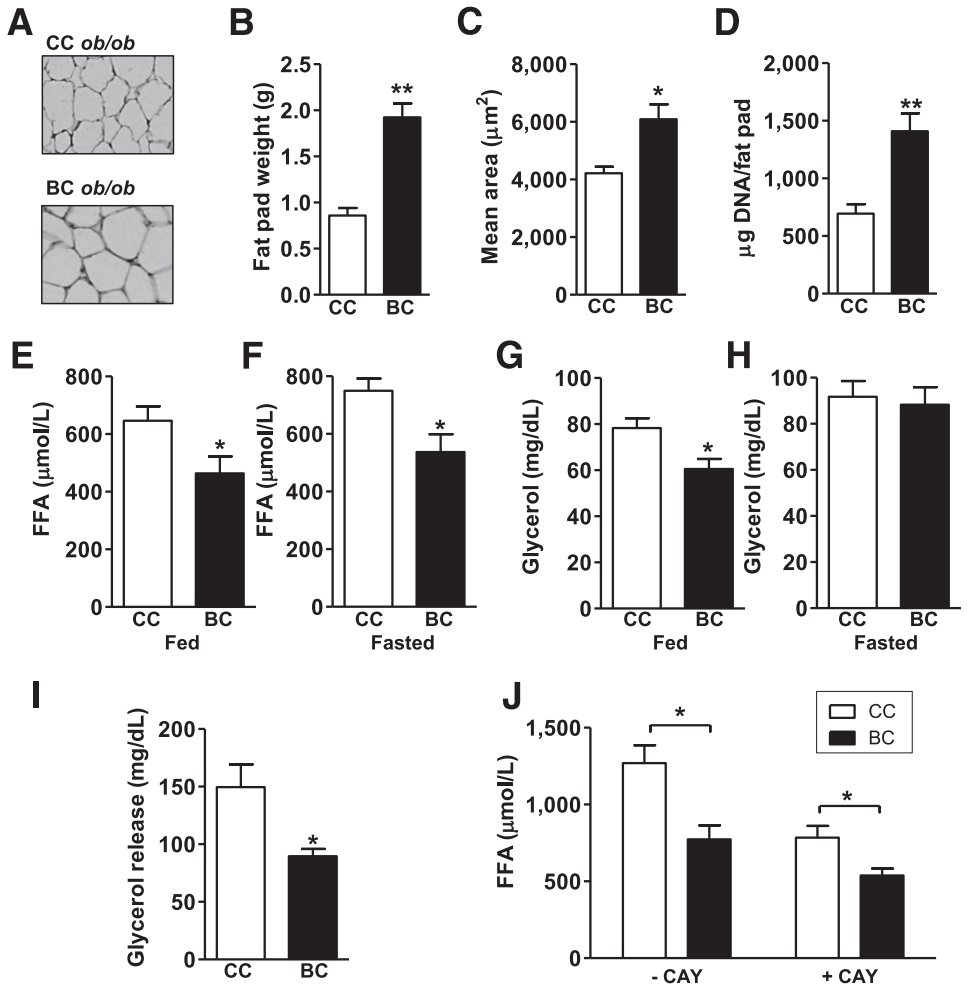

FIG. 2. BALB/c alleles promoted increased ATGL-mediated lipolysis. *A*: Histology (hematoxylin and eosin staining) of inguinal fat pad of 2-month-old BALB.2^{CC} and BALB.2^{BC} *ob/ob* mice. *B*: Average inguinal fat pad weight. *C*: The mean area of adipocytes was determined (>100 cells per animal; n = 6). *D*: Cell number per fat pad and per mouse were expressed in DNA content (n = 6). Determination of FFA (*E*, *F*) in plasma from fed and fasted congenic mice and glycerol concentrations (*G*, *H*) in serum from fed and fasted BALB.2^{CC} and BALB.2^{BC} *ob/ob* females (n = 6). *I*: Glycerol release from adipose tissue explants of BALB.2 ^{CC} and BALB.2^{BC} *ob/ob* mice under basal condition (n = 6). *J*: FFA release from BALB.2^{CC} and BALB.2^{BC}*ob/ob* adipose tissue explants in basal (−CAY) or in presence (+CAY) of the HSL inhibitor CAY10499. Five mice in each group were studied and analysis was performed in triplicate. Data are expressed as mean ± SEM. Unpaired t tests were performed. *P < 0.05. **P < 0.005.

Because only ATGL, and not HSL, was increased in parental (12) and in congenic lines, we assumed that at least ATGL might participate in BALB/c obesity resistance.

With RT quantitative PCR, we did not detect any difference in *Atgl* mRNA expression between BALB and B6 *ob/ob* (Fig. 3*A*), whereas ATGL protein was upregulated in WAT of BALB *ob/ob* (Fig. 3*B*) (12). In the adipose tissue of the congenic BALB.2^{BC} *ob/ob* strain, *Atgl* mRNA was downregulated by ~30% (Fig. 3*C*), whereas the ATGL protein level was decreased by ~70% (Fig. 3*D*). Unchanged or subtle alteration of *Atgl* mRNA suggests that a degradative mechanism could be involved in the regulation of ATGL protein expression (24). To assess ATGL protein stability, inguinal fat explants were cultured with or without CHX, an inhibitor of protein translation (25), and degradation of ATGL was followed by Western blot. In B6 *ob/ob* explants, ATGL was decreased by 50% after 5 h of incubation with CHX, whereas in BALB *ob/ob* adipose tissue the ATGL levels were unaffected (Fig. 3*E*). Similarly, in the congenic fat explants, inhibition of protein translation showed that ATGL was more rapidly degraded in BALB.2^{BC} *ob/ob* WAT as compared with BALB.2^{CC} (Fig. 3*F*). This difference in stability is likely to be involved in the difference in ATGL protein levels between BALB versus B6 *ob/ob* mice and between BALB.2^{CC} versus BALB.2^{BC} *ob/ob*. Then, we selectively inhibited the proteasome-mediated degradation in B6 fat explants using MG-132 (26) and found that the degradation of ATGL was suppressed in B6 and in BALB.2^{BC} *ob/ob* WAT explants in presence of MG-132 (Fig. 3*G–H*). Together, our data highlight that BALB/c alleles on chromosome 2 participate in ATGL protein levels in adipose tissue of leptin-deficient mice through a post-translational control involving the proteasomal degradation system.

BALB alleles exert a cell-autonomous role and limit the adipogenic competency. Decreased adipocyte number per fat pad in BALB.2^{CC} *ob/ob* mice indicated that hypoplasia contributed to the decreased fat mass. Consequently, we examined whether the BALB/c genome modified adipogenesis. Because new adipocytes can arise from a committed population of cells residing within the adipose tissue, we cultured and differentiated SV preadipocytes isolated from adipose tissue of lean BALB/c and B6 mice, as well as lean BALB.2^{CC} and BALB.2^{BC}congenic mice (Fig. 4). In response to the adipogenic cocktail, B6

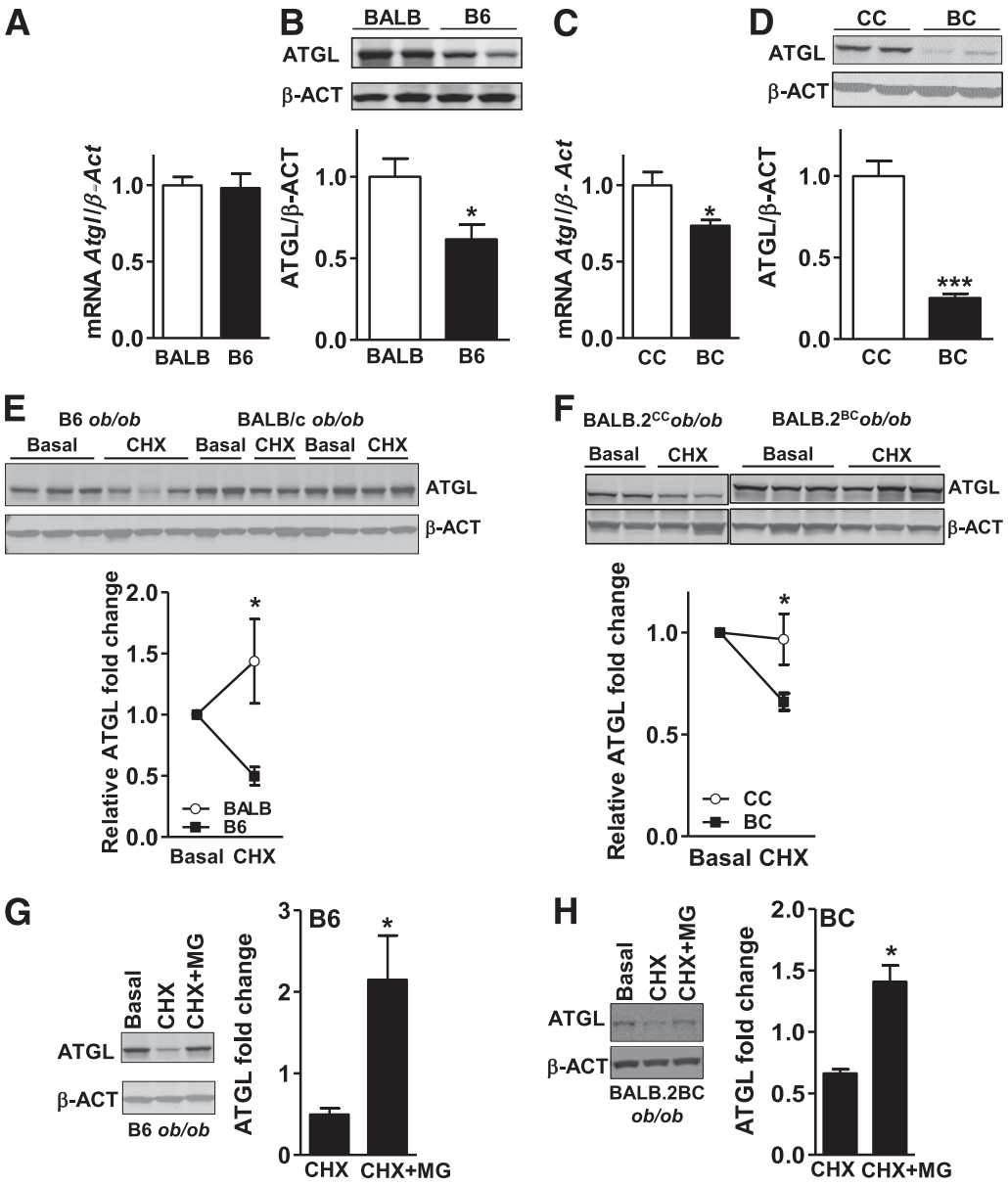

FIG. 3. BALB/c alleles enhanced ATGL protein stability. *A*: Quantification by RT quantitative PCR of *Atgl* mRNA in inguinal fat pad normalized to β-Actin (β-Act) expression in BALB and B6 *ob/ob* (n = 6). *B*: Immunoblot and densitometry analysis of ATGL in inguinal fat from BALB/c and B6 *ob/ob* (n = 3). *Atgl* mRNA quantification (*C*) and ATGL protein levels (*D*) in inguinal fat pad of BALB.2^{CC} and BALB.2^{BC} *ob/ob* (n = 6). Immunoblots and densitometry analysis of ATGL in (*E*) BALB/c and B6 *ob/ob* adipose tissue (AT; n = 4) or in (*F*) BALB.2^{CC} and BALB.2^{BC} *ob/ob* AT culture explants in basal conditions or when treated with CHX for 5 h (n = 3). ATGL fold change was calculated relative to basal condition. ATGL protein level analysis in (*G*) B6 *ob/ob* AT and (*H*) BALB.2^{BC}*ob/ob* AT culture during basal conditions, treated with CHX, or treated with CHX and MG-132 (n = 3). ATGL fold change was relative to basal ATGL level. Data are expressed as average ± SEM. Unpaired t tests were performed. *$P < 0.05$. ***$P < 0.0005$.

and BALB/c preadipocytes underwent morphological conversion into adipocytes, as evidenced by the accumulation of lipid stained with oil red O (Fig. 4*A*). However, adipogenesis of BALB/c preadipocytes was less efficient than in B6, because we counted fewer mature adipocytes (Fig. 4*C*). Similarly, BALB.2^{CC} preadipocytes also displayed reduced adipogenic potential (Fig. 4*B* and *D*). Accordingly, gene expression analysis showed that *Pparγ* and the differentiation markers (i.e., not expressed in preadipocytes) *Ap2*, *Atgl*, and *Hsl* were induced to higher levels in B6 relative to BALB/c cells (Fig. 4*E*), reflecting the increased B6 adipocyte count. These same observations were made for the cells derived from the congenic strains, with higher expression of *PPARγ*, *Ap2*, *Atgl*, and *Hsl* in BALB.2^{BC} cells relative to BALB.2^{CC} cells (Fig. 4*F*). When we compared the expression of the adipogenic regulator PPARγ in adipose tissue of BALB and B6 *ob/ob* mice, we did not find a trend toward decreased protein levels (1 ± 0.03 vs. 0.77 ± 0.08; P = 0.08). However, PPARγ also can be influenced by multiple factors such as the increased insulin concentration we observed in serum of BALB.2^{CC} congenic. In rodents, PPARγ expression is decreased by fasting and by insulin deficiency in adipose tissue, and treatment of diabetic mice with insulin leads to a partial restoration of PPARγ levels (27). Consequently, BALB/c alleles on chromosome 2 exert a cell-autonomous role to limit the adipogenic propensity that may contribute to decreased fat mass.

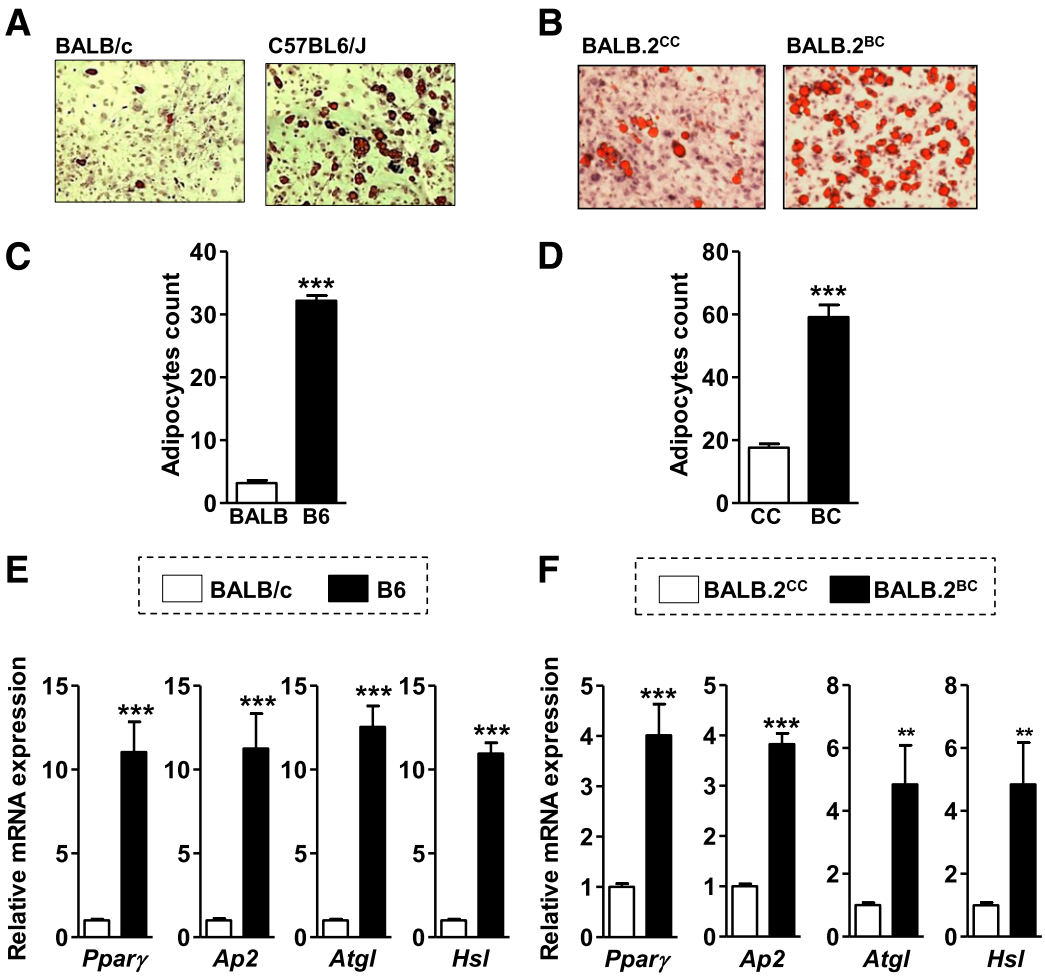

FIG. 4. Decreased adipocyte differentiation in BALB/c SV preadipocytes. Neutral lipid staining with oil red O in adipocytes on day 7 postdifferentiation induction in (*A*) BALB/c and B6 cells or in (*B*) BALB.2^{CC} and BALB.2^{BC} cells. Determination of the number of oil red O–stained adipocytes per field in (*C*) BALB/c and B6 cells or in (*D*) BALB.2^{CC} and BALB.2^{BC} cells (n = 5). mRNA expression analysis by quantitative RT-PCR of *Pparγ*, *Ap2*, *Atgl*, and *Hsl* normalized to *Actin* in (*E*) BALB/c and B6 cells or in (*F*) BALB.2^{CC} and BALB.2^{BC} cells (n = 5). Unpaired t tests were performed. **P < 0.005. ***P < 0.0005.

Identification of a nonsynonymous coding SNP in *Ube2l6* located in the *Lipq1* critical interval. The generation of subcongenic mice enabled us to narrow the position of the genes responsible for the obesity QTL on chromosome 2. We obtained subcongenic strains that contain a small introgressed region from the B6 chromosome 2 in the BALB/c background by crossing BALB.2^{BC} *ob*/+ and BALB.2^{CC} *ob*/+. Then, for each subcongenic strains, we determined the B6/BALB boundaries as well as the body fat fraction. Using this approach, we refined the location of the genes responsible for obesity resistance and narrowed the region to a 9.8-Mb interval on chromosome 2. The obese congenic strains BALB.2$^{BC79–123}$ and BALB.2$^{BC74–114}$ that carried the 9.8-Mb chromosome 2 segment derived from the C57BL6/J strain exhibited increased adiposity when compared with the obese congenic strains BALB.2$^{BC102–123}$, BALB.2$^{BC74–79}$, and BALB.2$^{BC89–123}$ (Fig. 5*A*). Because the subcongenic lines were at the fourth back-cross generation, some uncertainties regarding the remaining B6 contribution remained in the unmapped areas. Nevertheless, the probabilities of these results being observed because of the unmapped regions are very low because the unmapped regions would not be consistently inherited in the N4 cohorts, unlike the mapped introgressed region on chromosome 2.

We next used the complete genome sequence database (www.sanger.ac.uk) of C57BL6/J and BALB/c parental strains to identify putative candidates. There are 254 genes in the segment between 79.18 and 89 Mb on chromosome 2. Among them, we excluded from our analysis 37 putative genes and two microRNAs. We also excluded 186 genes (including 174 *Olfr* genes) that are not expressed in the adipose tissue of the *ob/ob* mice. Finally, we searched for expression variants between BALB/c and B6 among the 29 genes expressed in the adipose tissue and located on the chromosome 2 QTL. We observed only one gene *Frzb* with differential expression (Fig. 5*B*), but this was not confirmed by RT quantitative PCR in the obese congenic WAT (data not shown). We further investigated nonsynonymous coding SNPs (nsSNP) in genes expressed in WAT. Each nsSNP was categorized based on cross-species conservation and physicochemical properties, and a SIFT score (17) was assigned (Table 1). Interestingly, only *Ube2l6* was identified with a deleterious nsSNP between BALB and B6 strain. UBE2L6 is an ubiquitin-conjugating enzyme with a sequence that is well-conserved between E2 enzymes (28). In the B6 transcript, the guanine (codon #29 GAT) was replaced by a thymidine in the BALB/c sequence (*rs28011451*) (Figs. 5*C* and 6*A*). BALB/c polymorphism encodes a tyrosine in place of an aspartate conserved in

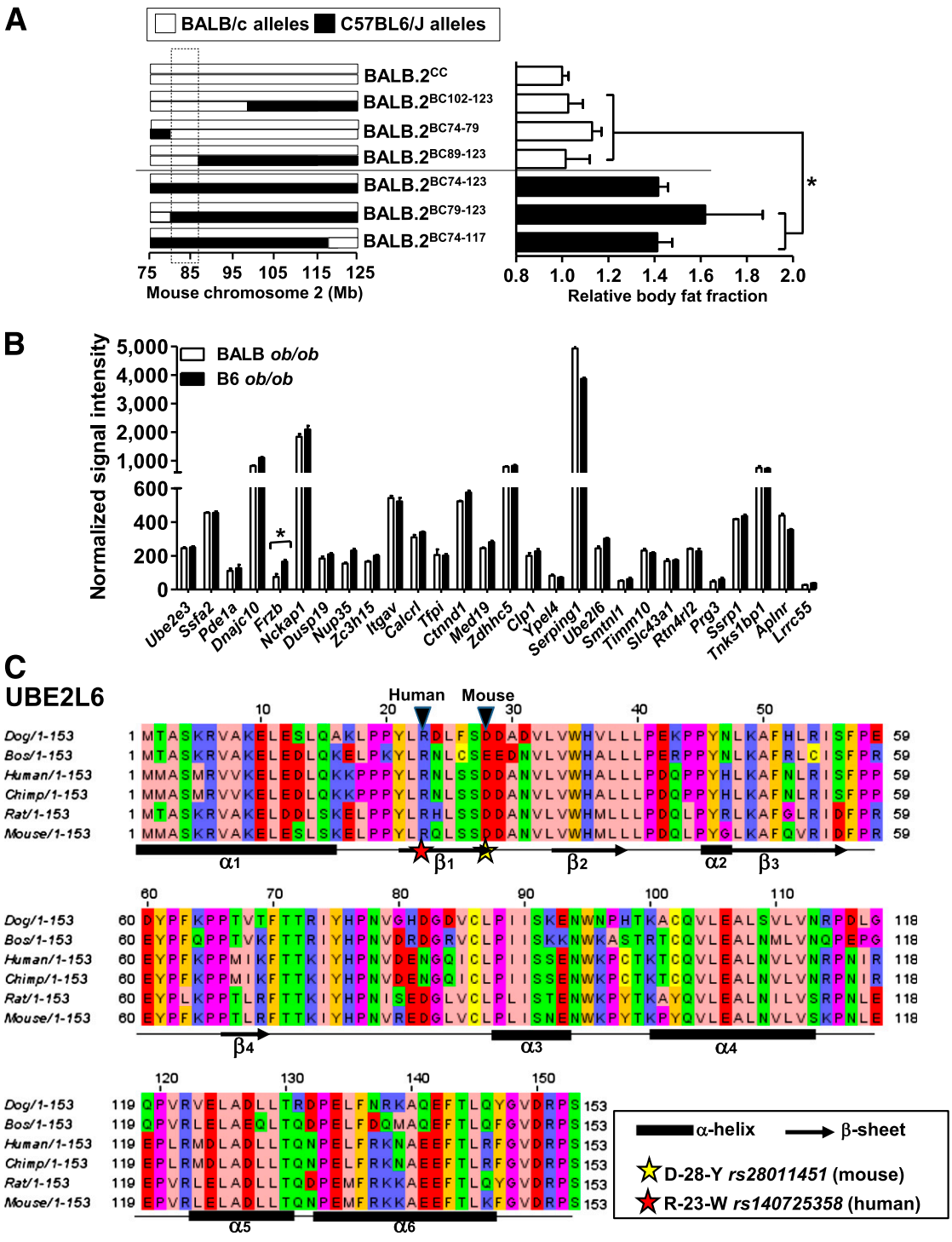

FIG. 5. Identification of a loss-of-function polymorphism in *Ube2l6* located in the narrowed chromosome 2 interval. *A*: On left, representation of the genotype of congenic mice generated by introgression of varying fragments of the B6 chromosome 2 into BALB/c mice. The indicated overlapping region of chromosome 2 shows the narrowed position of *Lipq1*. On right, fractional fat mass (relative to BALB.2^{CC}) of 2-month-old obese subcongenic mice ($n \geq 3$ in each genotype). *$P < 0.05$ for fractional fat mass of subcongenic mice including 1 copy of the 9.8-Mb fragment of B6 chromosome 2 compared with subcongenic mice including 2 copies of this 9.8-Mb region derived from BALB/c strain. *B*: Expression profiles of genes in the narrowed *Lipq1* was determined by microarray. *C*: Multiple protein sequence alignments of UBE2L6 protein in selected mammals show missense polymorphisms (indicated by an arrow head) at conserved residue in the mouse and human protein sequences. Secondary structural elements (α-helix and β-sheet) are indicated.

mammals (Fig. 5*C*). Thus, this substitution is likely to damage UBE2L6 protein.

The BALB/c allele of UBE2L6 is a hypomorphic variant. UBE2L6 protein is severely diminished in WAT and in confluent SV preadipocytes of BALB compared with B6 *ob/ob*, as well as in WAT of BALB.2^{CC} relative to BALB.2^{BC}*ob/ob* (Fig. 6*B*). We were able to amplify the full-length *Ube2l6*cDNA from BALB/c WAT (Fig. 6*C*), indicating that the coding sequence was unaltered. We subsequently assayed the consequence of the nsSNP on UBE2L6

TABLE 1
Genes with nonsynonymous coding SNP in the narrowed *Lipq1*

Gene symbol	Gene name	Position (Mb)	SNP ntB6→ntBALB*	Residues aaB6→aaBALB (position in protein)	Residue conserved†	Polymorphism conserved between mammals†	SIFT score‡
SSfa2	Sperm-specific antigen 2	79.48	A → G	Thr→ Ala (319)	Low	Yes	0.76
		79.50	T → G	Ile → Met (1071)	Yes	Yes	1
Frzb	Frizzled-related protein	80.25	G → A	Ala→ Val (321)	Yes	No	0.3
Dusp19	Dual-specificity phosphatase 19	80.47	G → C	Gly→ Asp (218)	No		1
		80.47	G → A	Gly → Arg (218)	No		0.49
Itgav	Integrin α/V	83.63	C → G	Ala→ Gly (872)	No		0.41
		83.64	G → T	Ala → Ser (921)	Yes	No	0.11
Serping1	Serine (or cysteine) peptidase inhibitor, clade G, member 1	84.61	A → G	Cys→ Arg (291)	Yes	Yes	1
Ube2l6	Ubiquitin-conjugating enzyme E2L 6	84.64	G → T	Asp →Tyr (29)	Yes	No	0.00
Tnks1bp1	Tankyrase 1-binding protein 1	84.89	C → G	Pro → Ala (351)	Yes	No	0.55
		84.89	C → T	Ala → Val (619)	Yes	Yes	0.43
		84.90	A → G	Asn → Asp (941)	Low	Yes	0.69

*Mouse Genomes Project, www.sanger.ac.uk. †Protein sequences at www.ensembl.org and conservation analysis with Jalview software (50). ‡SIFT score predicts whether an amino acid substitution will affect protein function. SIFT scores are classified as damaging if the score ranges from 0.00–0.05, as potentially intolerant if score ranges from 0.051–0.10, as borderline if score ranges from 0.101–0.2, or as tolerant if score ranges from 0.201–1.00 (17).

protein stability. We transfected 3T3-L1 fibroblasts with the BALB or the B6 variant of *Ube2l6* fused to a FLAG tag. The BALB Y28-UBE2L6 protein was markedly less expressed than the B6 D28-UBE2L6 (Fig. 6*D*) despite the same transfection efficiency (data not shown). Then, the stability of Y28-UBE2L6 and D28-UBE2L6 was determined in B16 cells treated with CHX. After 2 h, Y28-UBE2L6 protein started to decline, whereas unchanged amounts of D28-UBE2L6 were observed after 8 h of CHX (Fig. 6*E*). Consequently, the D-28-Y SNP compromised the stability of UBE2L6, explaining the loss of UBE2L6 protein in BALB/c tissues.

Knockdown of *Ube2l6* blocks 3T3-L1 cell lipid accumulation. To gain insight into the function of UBE2L6 in adipocyte physiology, we monitored UBE2L6 expression in WAT from lean and *ob/ob* C57BL6/J mice. UBE2L6 mRNA (data not shown) and protein levels were markedly decreased in WAT of leptin-deficient mice (Fig. 6*F*), suggesting that UBE2L6 expression was responsive to the metabolic changes. Also, UBE2L6 protein expression decreased during the early stage of 3T3-L1 adipogenesis (Fig. 6*G*). Together, these data suggest that *Ube2l6* may be related to the adipogenic process.

To characterize UBE2L6 function, we examined 3T3-L1 adipocytes with downregulated UBE2L6 expression. The 3T3-L1 cells, expressing the D28-UBE2L6 allele, were stably infected with a lentiviral vector expressing a scrambled siRNA or a siRNA targeting *Ube2l6*. We first confirmed that UBE2L6 protein was significantly decreased (~50%) in sh*Ube2l6* cells (Fig. 7*A*). After adipogenic induction, we qualitatively assessed the effect of *Ube2l6* knockdown on adipogenesis by performing oil red O staining of adipocytes (Fig. 7*B*) and observed that adipocyte number was markedly decreased in sh*Ube2l6* cells compared with sh*Control* adipocytes (Fig. 7*C*). Moreover, cellular TGs were measured to confirm the decreased lipid accumulation in sh*Ube2l6* adipocytes compared with controls (Fig. 7*D*). PPARγ was induced in sh*Ube2l6* adipocytes but to a lesser extent than in controls (Fig. 7*E*), suggesting that the UBE2L6 deficiency affected the differentiation program. We also analyzed markers of adipocytes (i.e., not expressed in preadipocytes) and found a significant decrease in aP2, ATGL, and HSL in sh*Ube2l6* cells attributable to lower adipocyte count (Fig. 7*F*). Overall, these findings were in accordance with our data reported because we found that BALB/c and BALB.2^{CC} SV preadipocytes had a reduced adipogenic propensity as the *shUbe2l6* cells. Thus, in BALB/c strain, we have characterized a deleterious mutation in *Ube2l6* and have shown that *Ube2l6* knockdown in 3T3-L1 recapitulated some aspects of BALB.2^{CC} *ob/ob* WAT that may contribute to adipocyte hypoplasia in fat pads.

DISCUSSION

In this report, we used congenic mice to uncover the genetic determinants located at the *Lipq1* locus on mouse chromosome 2 that protect BALB/c mice from obesity and glucose intolerance.

At the phenotypic level, our data revealed that the allelic variation in *Lipq1* limited fat mass expansion via two mechanisms. First, we observed heightened lipolysis rates that would control adipocyte TG content (29,30) and adipocyte size. This was concomitant with an increase in ATGL-mediated TG breakdown and prolongation of ATGL half-life in adipose tissue. This process is likely relevant to human obesity because obese individuals have been shown to present increased *Atgl* mRNA expression in subcutaneous adipose tissue, whereas ATGL protein was decreased in this depot compared with lean individuals (31). Thus, discrepancy between mRNA and protein expression may reflect posttranslational mechanisms such as

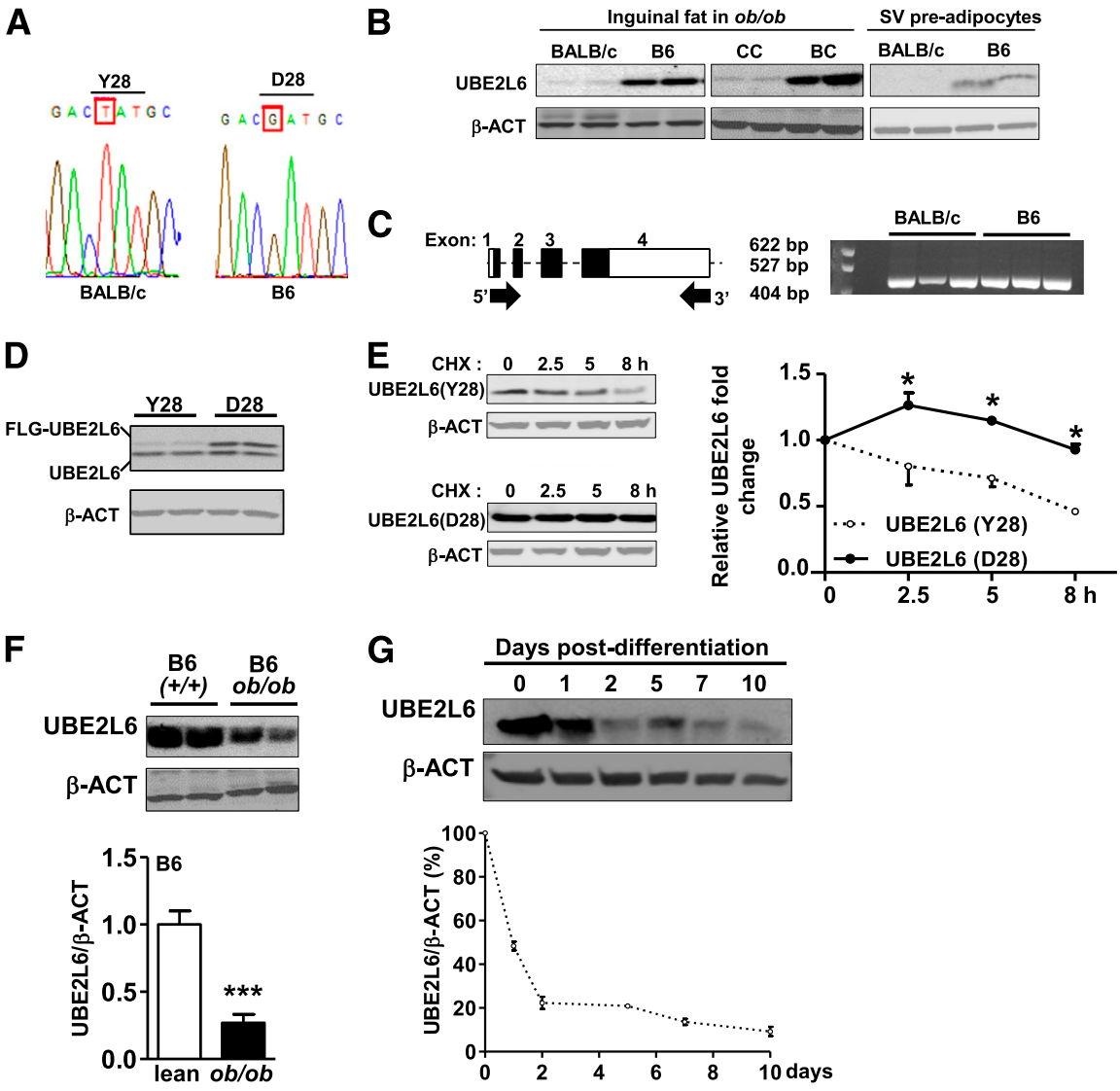

FIG. 6. BALB/c allele of UBE2L6 is a hypomorph and UBE2L6 expression is repressed during obesity and 3T3 adipogenesis. *A*: BALB/c and B6 polymorphism detection in DNA sequence electropherogram. The aspartate (D) substitution to tyrosine(Y) is indicated. *B*: Immunoblot and densitometry analysis of UBE2L6 in inguinal fat from BALB/c and B6 *ob/ob* ($n = 4$), in inguinal fat from BALB.2^{CC} and BALB.2^{BC} *ob/ob* ($n = 3$), and in SV preadipocytes from lean BALB/c and B6 mice, at day 0, before addition of the differentiating medium ($n = 3$). *C*: Cartoon representing the exon organization of *Ube2l6* transcript. Open boxes (□) show the 5′ and 3′ UTR and filled boxes (■) show the coding sequence. Whole *Ube2l6* transcript can be amplified from BALB and B6 *ob/ob* inguinal fat samples shown by gel electrophoresis. *D*: Immunoblots of UBE2L6 in 3T3 fibroblasts protein extracts prepared 48 h after transfection with BALB (Y28) or B6 (D28) FLAG-UBE2L6. *E*: Protein expression analysis of BALB (Y28) or B6 (D28) FLAG-UBE2L6 after incubation with the CHX for the indicated time ($n = 3$). Immunoblots and densitometry analysis of UBE2L6 (*F*) in inguinal fat from ($^{+/+}$) lean and *ob/ob* B6 mice ($n = 3$). *G*: UBE2L6 protein expression during differentiation of 3T3-L1 adipocytes ($n = 3$). Data are expressed as average ± SEM. Unpaired *t* tests were performed. *$P < 0.05$. ***$P < 0.0005$.

modification of protein stability between lean and obese human adipocytes as we observed in our model. Second, we found impaired adipogenic potential in preadipocytes bearing *Lipq1*, which would explain the decrease in mature adipocytes numbers we measured (11,32). Because altering the amount of ATGL activity does not alter adipocyte differentiation either in cell culture models or in vivo (29,30,33), it is unlikely that adipocyte numbers would be affected by the downregulation of ATGL we observed. The importance of adipocyte number and changes in adipose cellularity can be a major factor regulating fat pad size and obesity. Restraining adipogenic potential is associated with obesity resistance (34,35) and, conversely, adipocyte hyperplasia favors obesity (11,36).

In search of the putative candidate genes limiting obesity susceptibility in our model, we refined the obesity QTL and identified a missense coding polymorphism in *Ube2l6* encoding an E2 ubiquitin-conjugating enzyme. UBE2L6 is involved in ubiquitination of multiple substrates (37,38) and, like all E2 enzymes, it acts via selective interactions with E3 enzymes that confer specificity to ubiquitination by recognizing target substrates (39). Furthermore, UBE2L6 serves as the E2 enzyme for posttranslational addition of an ubiquitin-like protein ISG15 (interferon-stimulated gene 15) important for antiviral immunity (40,41), although we have not found ISG15 expression in WAT (data not shown). The critical role of UBE2L6 in BALB/c obesity resistance was strongly supported by several lines of evidence. First, *Ube2l6* is located in the 9.8-Mb minimal interval and harbors a polymorphism in BALB/c mice coding for a defective allele. This is in line with BALB/c obesity resistance, which is a recessive inherited

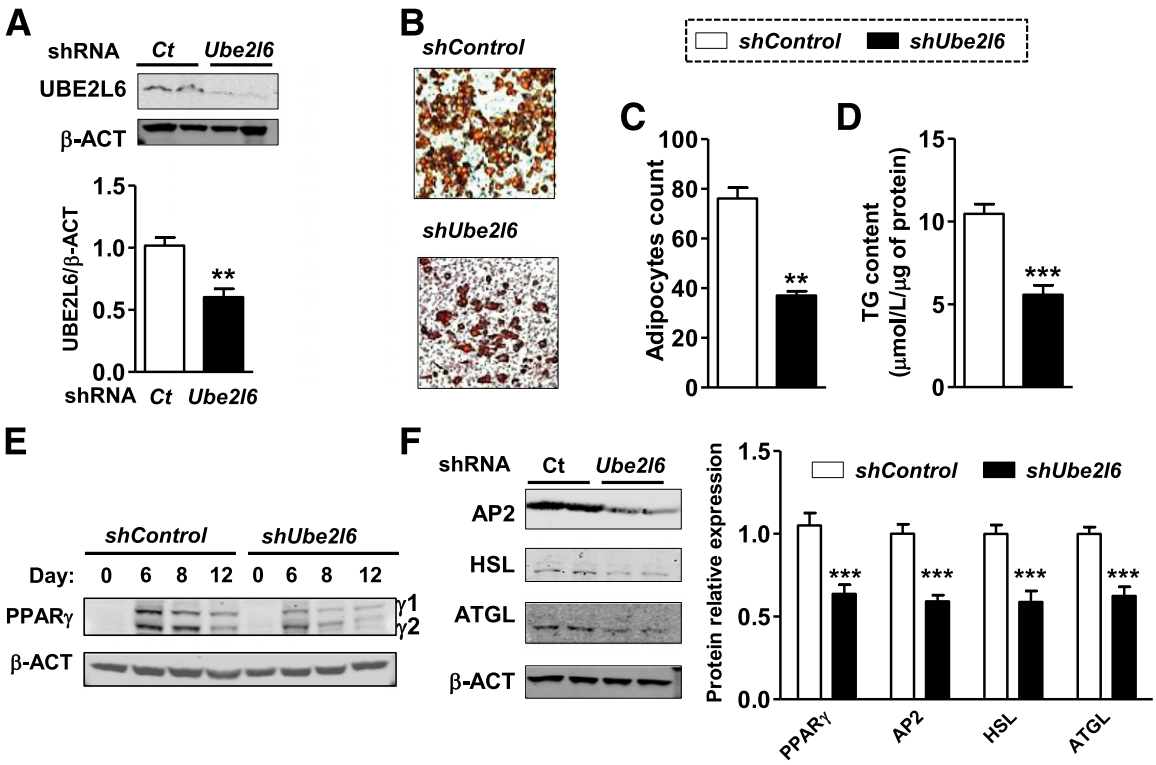

FIG. 7. Effects of UBE2L6 knockdown in 3T3 adipocytes. *A*: Immunoblots and densitometry analysis of UBE2L6 expression in 3T3 preadipocytes infected with sh*Control* or sh*Ube2l6* lentiviral particles (n = 4). *B*: Oil red O staining in adipocytes on day 12 postdifferentiation induction. *C*: Determination of the number of oil red O–stained adipocytes per field (n = 5). *D*: TG content in sh*Control* and sh*Ube2l6* adipocytes at day 12 normalized to protein quantity in each well (n = 6). *E*: PPARγ protein expression during 3T3 adipogenesis. *F*: Immunoblots of AP2, HSL, ATGL normalized with β-actin (β-ACT) in sh*Control* or sh*Ube2l6* adipocytes obtained at day 12 postdifferentiation. Quantification of protein expression level in sh*Control* and sh*Ube2l6* adipocytes at day 12 (n = 5). Data are expressed as average ± SEM. Unpaired t tests were performed. **$P < 0.005$. ***$P < 0.0005$. Ct, control.

trait. Also, the increased expression of UBE2L6 protein in lean versus obese adipose tissue indicated that UBE2L6 levels are regulated in response to metabolic changes. Finally, *Ube2l6* knockdown in 3T3-L1 adipocytes revealed that UBE2L6 was critically involved in adipocyte differentiation mirroring the impaired BALB/c and BALB.2^{CC} SV adipogenic potential. Consequently, UBE2L6 appeared to be a key regulator of adipocyte biology that likely determines obesity susceptibility in our model. It is intriguing that UBE2L6 expression and proteasomal degradation correlated with decreased ATGL stability in B6 adipose tissue. However, we were unable, so far, to detect any ubiquitination of ATGL using in vivo and in vitro ubiquitinylation assays (data not shown). In cells in which *Ube2l6* was knocked-down, inhibition of adipogenesis did not enable us to measure ATGL protein expression because of the differential degree of differentiation. Thus, further studies remain necessary to evaluate the link between UBE2L6 and ATGL protein regulation.

BALB/c obesity resistance was associated with improved glucose tolerance and insulin sensitivity, despite increased circulating levels of FFA. This result contrasted with the ATGL knockout mice characterized by decreased FFA and improved glucose tolerance and insulin sensitivity (42). However, we can hypothesize that decreased adiposity may counterbalance the effects of increased FFAs, as in transgenic mice overexpressing ATGL in the adipose tissue (29). In addition, BALB.2^{CC} *ob/ob* mice are characterized by increased insulin level. Although the reason why insulinemia increased is currently unknown, we can hypothesize that elevated FFA levels in the BALB.2^{CC} strain may contribute to increased insulin secretion (43).

The BALB/c-*Ube2l6* allele is found in several strains such as A/J, AKR/J, C3H/HeJ, CBA/J, DBA/2J, and LP/J, whereas the B6-*Ube2l6* allele is found in three 129/SV substrains, NOD strains, and NZO strains (www.sanger.ac.uk). Because BALB/c and DBA/2J, the first inbred mouse strain to be developed (44), share the same allele, it is likely that *Ube2l6* variants existed before the development of inbred mouse strains and its widespread representation would suggest that it is a functional variant that is advantageous under conditions of domestication (reliable food supply) to limit obesity. Of note, the wild strains CAST/EiJ, PWK/PhJ, Spretus/EiJ, and WSB/EiJ all have the C57BL6/J variant, suggesting that B6-*Ube2l6* variant promotes efficient storage in times of food abundance, providing a survival advantage during times of food shortage (45,46). Interestingly, the human UBE2L6 gene encodes the obesogenic polymorphism (D28) encoded by the C57BL/6 allele. However, the SNP database (47) lists genetic variation at the human *UBE2L6* locus. Notably, *rs140725358* located in the same domain as the mouse BALB/c polymorphism (Fig. 5*C*) is predicted to be highly deleterious by SIFT score, as was predicted for the BALB/c *Ube2l6* allele, although the very low frequency of this allele makes it a relatively rare allele. Thus, it would be interesting to investigate such variants as an obesity-protective polymorphism in humans.

Overall, our data support the implication of UBE2L6 in BALB/c obesity resistance. In vivo, BALB/c alleles

functions to decrease adipocyte size and number, and in vitro we found that BALB/c alleles repressed SV adipogenic potential. Similarly, limited adipogenesis led to decreased TG accumulation in 3T3-L1 adipocytes with *Ube2l6* knockdown. Thus, repressed adipogenic potential after *Ube2l6* knockdown would explain adipocyte hypoplasia in BALB/c mice. UBE2L6 is expressed in 3T3-L1 preadipocytes and its expression is suppressed early after addition of the differentiation medium, suggesting its important role during the very early stage of preadipocytics differentiation during growth arrest and commitment steps (48,49). Thus, using genetics, we identified a new gene controlling adipocyte commitment; however, future studies will be needed to identify UBE2L6 targets.

ACKNOWLEDGMENTS

This work was partly funded by a pilot grant from DK026687 (G.M.), RO1DK057621, PO1DK26687 (NYNORC: S.C.C., G.J.S.), HD058155 (S.C.C.), and DK020541 (EINSTEIN DRTC: G.J.S.).

No potential conflicts of interest relevant to this article were reported.

G.M. researched the data and wrote the manuscript. S.-M.L. researched the data. G.J.S. reviewed and edited the manuscript and contributed to discussion. S.C.C. reviewed and edited the manuscript and contributed to discussion. S.C.C. is the guarantor of this work and, as such, had full access to all the data in the study and takes responsibility for the integrity of the data and the accuracy of the data analysis.

This study was presented at the meeting of The Obesity Society, San Antonio, Texas, 20–24 September 2012.

The authors thank Merck Research Laboratory and Dr. Su Qian, Merck Research Laboratory, who provided the *AgrpKO* mouse model. The authors also thank Dr. Emmanuel Gautier (Washington University School of Medicine, St. Louis, Missouri) for his helpful discussion.

REFERENCES

1. Zechner R, Zimmermann R, Eichmann TO, et al. FAT SIGNALS—lipases and lipolysis in lipid metabolism and signaling. Cell Metab 2012;15:279–291
2. Landsberg L. Feast or famine: the sympathetic nervous system response to nutrient intake. Cell Mol Neurobiol 2006;26:497–508
3. Shen J, Tanida M, Niijima A, Nagai K. In vivo effects of leptin on autonomic nerve activity and lipolysis in rats. Neurosci Lett 2007;416:193–197
4. Buettner C, Muse ED, Cheng A, et al. Leptin controls adipose tissue lipogenesis via central, STAT3-independent mechanisms. Nat Med 2008;14:667–675
5. Marcelin G, Chua S Jr. Contributions of adipocyte lipid metabolism to body fat content and implications for the treatment of obesity. Curr Opin Pharmacol 2010;10:588–593
6. Kersten S. Mechanisms of nutritional and hormonal regulation of lipogenesis. EMBO Rep 2001;2:282–286
7. Turner SM, Roy S, Sul HS, et al. Dissociation between adipose tissue fluxes and lipogenic gene expression in ob/ob mice. Am J Physiol Endocrinol Metab 2007;292:E1101–E1109
8. Hausman DB, DiGirolamo M, Bartness TJ, Hausman GJ, Martin RJ. The biology of white adipocyte proliferation. Obes Rev 2001;2:239–254
9. Rodeheffer MS, Birsoy K, Friedman JM. Identification of white adipocyte progenitor cells in vivo. Cell 2008;135:240–249
10. Arner P. The adipocyte in insulin resistance: key molecules and the impact of the thiazolidinediones. Trends Endocrinol Metab 2003;14:137–145
11. Naaz A, Holsberger DR, Iwamoto GA, Nelson A, Kiyokawa H, Cooke PS. Loss of cyclin-dependent kinase inhibitors produces adipocyte hyperplasia and obesity. FASEB J 2004;18:1925–1927
12. Marcelin G, Liu SM, Li X, Schwartz GJ, Chua S. Genetic control of ATGL-mediated lipolysis modulates adipose triglyceride stores in leptin-deficient mice. J Lipid Res 2012;53:964–972
13. Cariou B, Postic C, Boudou P, et al. Cellular and molecular mechanisms of adipose tissue plasticity in muscle insulin receptor knockout mice. Endocrinology 2004;145:1926–1932
14. Satyanarayana A, Klarmann KD, Gavrilova O, Keller JR. Ablation of the transcriptional regulator Id1 enhances energy expenditure, increases insulin sensitivity, and protects against age and diet induced insulin resistance, and hepatosteatosis. FASEB J 2012;26:309–323
15. Fried SK, Zechner R. Cachectin/tumor necrosis factor decreases human adipose tissue lipoprotein lipase mRNA levels, synthesis, and activity. J Lipid Res 1989;30:1917–1923
16. Zechner R, Moser R, Newman TC, Fried SK, Breslow JL. Apolipoprotein E gene expression in mouse 3T3-L1 adipocytes and human adipose tissue and its regulation by differentiation and lipid content. J Biol Chem 1991; 266:10583–10588
17. Kumar P, Henikoff S, Ng PC. Predicting the effects of coding non-synonymous variants on protein function using the SIFT algorithm. Nat Protoc 2009;4: 1073–1081
18. Kim KI, Giannakopoulos NV, Virgin HW, Zhang DE. Interferon-inducible ubiquitin E2, Ubc8, is a conjugating enzyme for protein ISGylation. Mol Cell Biol 2004;24:9592–9600
19. Singh R, Xiang Y, Wang Y, et al. Autophagy regulates adipose mass and differentiation in mice. J Clin Invest 2009;119:3329–3339
20. Qian S, Chen H, Weingarth D, et al. Neither agouti-related protein nor neuropeptide Y is critically required for the regulation of energy homeostasis in mice. Mol Cell Biol 2002;22:5027–5035
21. Schweiger M, Schreiber R, Haemmerle G, et al. Adipose triglyceride lipase and hormone-sensitive lipase are the major enzymes in adipose tissue triacylglycerol catabolism. J Biol Chem 2006;281:40236–40241
22. Grisouard J, Bouillet E, Timper K, et al. Both inflammatory and classical lipolytic pathways are involved in lipopolysaccharide-induced lipolysis in human adipocytes. Innate Immun 2012;18:25–34
23. Noyes HA, Agaba M, Anderson S, et al. Genotype and expression analysis of two inbred mouse strains and two derived congenic strains suggest that most gene expression is trans regulated and sensitive to genetic background. BMC Genomics 2010;11:361
24. Ciechanover A, Schwartz AL. The ubiquitin-proteasome pathway: the complexity and myriad functions of proteins death. Proc Natl Acad Sci USA 1998;95:2727–2730
25. Schneider-Poetsch T, Ju J, Eyler DE, et al. Inhibition of eukaryotic translation elongation by cycloheximide and lactimidomycin. Nat Chem Biol 2010;6:209–217
26. Lee DH, Goldberg AL. Proteasome inhibitors: valuable new tools for cell biologists. Trends Cell Biol 1998;8:397–403
27. Vidal-Puig A, Jimenez-Liñan M, Lowell BB, et al. Regulation of PPAR gamma gene expression by nutrition and obesity in rodents. J Clin Invest 1996;97:2553–2561
28. Serniwka SA, Shaw GS. The structure of the UbcH8-ubiquitin complex shows a unique ubiquitin interaction site. Biochemistry 2009;48:12169–12179
29. Ahmadian M, Duncan RE, Varady KA, et al. Adipose overexpression of desnutrin promotes fatty acid use and attenuates diet-induced obesity. Diabetes 2009;58:855–866
30. Smirnova E, Goldberg EB, Makarova KS, Lin L, Brown WJ, Jackson CL. ATGL has a key role in lipid droplet/adiposome degradation in mammalian cells. EMBO Rep 2006;7:106–113
31. Steinberg GR, Kemp BE, Watt MJ. Adipocyte triglyceride lipase expression in human obesity. Am J Physiol Endocrinol Metab 2007;293:E958–E964
32. Jones JR, Barrick C, Kim KA, et al. Deletion of PPARgamma in adipose tissues of mice protects against high fat diet-induced obesity and insulin resistance. Proc Natl Acad Sci USA 2005;102:6207–6212
33. Kershaw EE, Hamm JK, Verhagen LA, Peroni O, Katic M, Flier JS. Adipose triglyceride lipase: function, regulation by insulin, and comparison with adiponutrin. Diabetes 2006;55:148–157
34. Wolfrum C, Shih DQ, Kuwajima S, Norris AW, Kahn CR, Stoffel M. Role of Foxa-2 in adipocyte metabolism and differentiation. J Clin Invest 2003;112: 345–356
35. Blüher M, Michael MD, Peroni OD, et al. Adipose tissue selective insulin receptor knockout protects against obesity and obesity-related glucose intolerance. Dev Cell 2002;3:25–38
36. Kim JY, van de Wall E, Laplante M, et al. Obesity-associated improvements in metabolic profile through expansion of adipose tissue. J Clin Invest 2007;117:2621–2637
37. Buchwald M, Pietschmann K, Müller JP, Böhmer FD, Heinzel T, Krämer OH. Ubiquitin conjugase UBCH8 targets active FMS-like tyrosine kinase 3 for proteasomal degradation. Leukemia 2010;24:1412–1421
38. Shibata E, Abbas T, Huang X, Wohlschlegel JA, Dutta A. Selective ubiquitylation of p21 and Cdt1 by UBCH8 and UBE2G ubiquitin-conjugating enzymes via the CRL4Cdt2 ubiquitin ligase complex. Mol Cell Biol 2011;31: 3136–3145
39. van Wijk SJ, Timmers HT. The family of ubiquitin-conjugating enzymes (E2s): deciding between life and death of proteins. FASEB J 2010;24:981–993

40. Skaug B, Chen ZJ. Emerging role of ISG15 in antiviral immunity. Cell 2010; 143:187–190
41. Zhao C, Beaudenon SL, Kelley ML, et al. The UbcH8 ubiquitin E2 enzyme is also the E2 enzyme for ISG15, an IFN-alpha/beta-induced ubiquitin-like protein. Proc Natl Acad Sci USA 2004;101:7578–7582
42. Haemmerle G, Lass A, Zimmermann R, et al. Defective lipolysis and altered energy metabolism in mice lacking adipose triglyceride lipase. Science 2006;312:734–737
43. Itoh Y, Kawamata Y, Harada M, et al. Free fatty acids regulate insulin secretion from pancreatic beta cells through GPR40. Nature 2003;422:173–176
44. Little CC, Tyzzer EE. Further experimental studies on the inheritance of susceptibility to a Transplantable tumor, Carcinoma (J. W. A.) of the Japanese waltzing Mouse. J Med Res 1916;33:393–453
45. Coleman DL. Obesity genes: beneficial effects in heterozygous mice. Science 1979;203:663–665
46. Chung WK, Belfi K, Chua M, et al. Heterozygosity for Lep(ob) or Lep(rdb) affects body composition and leptin homeostasis in adult mice. Am J Physiol 1998;274:R985–R990
47. Sherry ST, Ward MH, Kholodov M, et al. dbSNP: the NCBI database of genetic variation. Nucleic Acids Res 2001;29:308–311
48. Ntambi JM, Young-Cheul K. Adipocyte differentiation and gene expression. J Nutr 2000;130:3122S–3126S
49. Rosen ED, Walkey CJ, Puigserver P, Spiegelman BM. Transcriptional regulation of adipogenesis. Genes Dev 2000;14:1293–1307
50. Waterhouse AM, Procter JB, Martin DM, Clamp M, Barton GJ. Jalview Version 2—a multiple sequence alignment editor and analysis workbench. Bioinformatics 2009;25:1189–1191